

# Influence of Sulfuric Acid Bath on Morphological Structure and Mechanical Properties of Poly(*p*-phenylene-1,3,4-oxadiazole) Fibers

Zaixing Zhang, Guangdou Ye, Wentao Li, Ting Li, Jianjun Xu

State Key Laboratory of Polymer Materials Engineering, College of Polymer Science and Engineering, Sichuan University, Sichuan 610065, Chengdu, China

Received 12 November 2008; accepted 9 April 2009

DOI 10.1002/app.30671

Published online 23 June 2009 in Wiley InterScience (www.interscience.wiley.com).

**ABSTRACT:** Poly(*p*-phenylene-1,3,4-oxadiazoles) (*p*-PODs) spinning solution was prepared by one-step polycondensation, and *p*-POD fibers were obtained by wet spinning method using dilute sulfuric acid as coagulation bath. The morphology and mechanical properties of *p*-POD fibers under different coagulating conditions, such as bath concentration and temperature, were qualitatively and quantitatively studied by microscopes, ultrasonic orientation measurement, WAXD, and other traditional methods. The microscopic observation indicated that the *p*-POD fibers were of three-layer structure which consisted of outer skin, inner skin, and the core. The skin-core structure and surface feature of the fibers were greatly affected by the coagulating conditions. At the same time, the results of WAXD and ultrasonic orientation measurement demon-

strated that the crystallinity and orientation of the fibers also varied with the change of bath conditions. The tests of mechanical properties showed that the tensile strength, elongation at break, and maximum draw ratio of the *p*-POD fibers were determined by their solid-phase structures, which were largely influenced by coagulation conditions. According to the structure analysis and the mechanical tests, the optimal coagulation parameters were chosen to obtain *p*-POD fibers with denser and more regular structure and better mechanical properties. © 2009 Wiley Periodicals, Inc. *J Appl Polym Sci* 114: 1485–1493, 2009

**Key words:** poly(*p*-phenylene-1,3,4-oxadiazole) fiber; wet spinning; coagulation condition; morphological structure; mechanical properties

## INTRODUCTION

Aromatic poly(1,3,4-oxadiazole)s (PODs) are a class of heterocyclic polymers with excellent thermal stability, good chemical stability, high glass transition temperatures, low dielectric constants, and tough mechanical properties,<sup>1,2</sup> which had been extensively studied for a long time. And great interests have been continually attracted in the preparation of high-performance materials. These kinds of polymers exhibit fine fiber- and film-forming abilities, and thus can be processed into fibers, special membranes, and photoelectric materials. The fibers can be used for heat-resistant composite materials, filtration fabrics, and protective working clothes, and the special membranes may be used for gas separation or reverse osmosis.<sup>1</sup> So far there have been two practical ways for PODs polycondensation, namely the two-step and the one-step polymerization method.<sup>1,3,4</sup> In the two-step method, the polyhy-

drazides (PHs) were first synthesized, and then cyclodehydrated at high temperatures under vacuum or under nitrogen atmosphere for long periods.<sup>5</sup> In the one-step method, PODs were formed by polycondensation in aggressive reaction media such as oleum, polyphosphoric acid (PPA), and phosphorus pentoxide/methanesulfonic acid (PPMA).<sup>6,7</sup> The latter is more feasible to control, and the final products like films and fibers are compact and have good mechanical properties.<sup>1</sup>

Although one-step method is convenient to polymerize PODs, few commercial products are obtained by this method, except Oxalon made in Russia.<sup>8</sup> Several studies have shown that PODs synthesized via one-step method could fabricate the POD fibers by wet spinning or dry jet-wet spinning (DJWS). The mechanical properties of POD fibers are apparently affected by the spinning, coagulating, stretching, and post-treatment conditions.<sup>9–12</sup> However, researches on the influence of the coagulation bath on the POD fiber's morphological formation and mechanical properties have rarely been reported.

The aim of this work is to reveal how the coagulating conditions influence the morphological structure and mechanical properties of the *p*-POD fiber, and to develop a feasible way for producing the

Correspondence to: J. Xu (xujj@scu.edu.cn).

Contract grant sponsor: The National Natural Science Foundation of China; contract grant number: 50873061.

POD fiber or film via POD solutions by one-step method.

## EXPERIMENTAL

### Materials

Terephthalic acid (TPA), 20% fuming sulfuric acid, 96% sulfuric acid and benzoic acid were analytical grade, and were used as received. Hydrazine sulfate (HS) with chemical grade was purified by recrystallization from distilled water for twice. TPA and purified HS were dried in vacuum oven at 80°C for 12 h before use.

### Synthesis of poly(*p*-phenylene-1,3,4-oxadiazole)s

In the synthesis of poly(*p*-phenylene-1,3,4-oxadiazole)s TPA and HS were used as monomers, and 20% fuming sulfuric acid as solvent and condensing agent. The molar ratio of SO<sub>3</sub>/TPA and HS/TPA were 4 : 1 and 1.05 : 1, respectively. The concentration of TPA was 1.0 mol in all polymerizations.

One sample of polymer was prepared by the one-step method with two stages described by Iwakura,<sup>6</sup> and the other sample was obtained by the one-step method with three stages, which was recently developed by our group.<sup>13</sup> The samples were coded as *L-p*-POD and *H-p*-POD, respectively (as seen in Table I).

After the reaction was completed, most of the polymer solution was filtered and deaerated for spinning. The rest of the solution was isolated in distilled water and purified by decantation with water for 48 h to remove sulfuric acid and other residuals. After drying, the *p*-PODs resins were further dehydrated in vacuum oven at 110°C for 2 h for WAXD measurements and titrimetric analysis of coagulability.

### Preparation of fiber samples

The spinning solution (about 80°C) was passed from the acid-resistant supply vessel to a metering pump with a volume of 0.6 mL rpm, and sent to a stainless steel spinneret with 30 orifices which had a diameter of 0.20 mm, and then extruded into an 80 cm length of coagulating bath at different sulfuric acid concentrations (0–50 wt %) and temperatures (30–80°C).

**TABLE I**  
Intrinsic Viscosities and Elemental Contents of *L-p*-POD and *H-p*-POD

Samples	Intrinsic viscosity (dL g <sup>-1</sup> )	Solid content (wt %)	Elemental content (%)				%CD
			N	C	H	O	
<i>L-p</i> -POD	1.89	8.05	18.55	63.83	3.26	14.59	59.7
<i>H-p</i> -POD	1.69	7.86	18.88	64.59	3.39	13.14	76.5

The extrusion speed of the spinning solution was 3.0 m min<sup>-1</sup>. The filament coagulated was taken up by rollers and reached a collector bobbin. The drawn samples and nondrawn samples (as-spun fibers) were obtained. The nonoriented samples were obtained by freely extruding the spinning solution into the coagulation bath of certain concentration and temperature, and the standard nonoriented sample was obtained in 50% H<sub>2</sub>SO<sub>4</sub> solution at 5°C. All samples were washed for 48 h with running water, and purified by being dipped into dilute sodium bicarbonate and acetone solution for 2 h, respectively. They were then washed in distilled water for 5 times, and finally dried at 110°C.

### Characterization and measurements

The intrinsic viscosities [η] of the *p*-POD samples were determined with an Ubbelohde viscometer (the diameter was 0.90 mm, and the solution concentration was 0.3–0.5 g dL<sup>-1</sup>) at 30°C in 96% sulfuric acid.

Elemental analysis was carried out on a standard Flash EA 1112 apparatus (Thermo Quest Italia). Because of the hygroscopic nature of PODs,<sup>5</sup> all samples were dried in a vacuum oven at 110°C for 2 h, weighed as original weights, and kept in a desiccator before measurement. In terms of the content of C, H, and N, the content of O was computed. The cyclization degree (%CD) of the *p*-POD fibers was got from the eq. (1)<sup>5,13</sup>:

$$\%CD = \frac{19.75 - O_{\text{POD}}}{19.75 - 11.11} \times 100 \quad (1)$$

where 19.75% is the oxygen content of poly(*p*-phenylene hydrazide) without cyclodehydration, and 11.11% is the oxygen content of *p*-POD with 100% cyclodehydration. O<sub>POD</sub> is the actual oxygen content of the *p*-POD samples obtained under different reaction conditions.

Wide-angle X-ray diffraction (WAXD) measurements were performed at room temperature on a X'Pert Pro (Philips) X-ray diffractometer operating in the 2θ range of 10–45° (for filament) or 10–40° (for powder) at a scanning rate of 12° per minute with nickel-filtered Cu Kα radiation.

The orientation measurements of the fibers were performed by SCY-III Ultrasonic orientation measurement apparatus (Donghua University, China). The ultrasound speed of the standard nonoriented sample was 1.256 Km s<sup>-1</sup>. The orientation factors are calculated from the eq. (2)<sup>14</sup>:

$$f = 1 - \left( \frac{v_0}{v_1} \right)^2 \quad (2)$$

Here *f* is the orientation factor, *v*<sub>0</sub> is the acoustic speed of the standard nonoriented *p*-POD fiber,

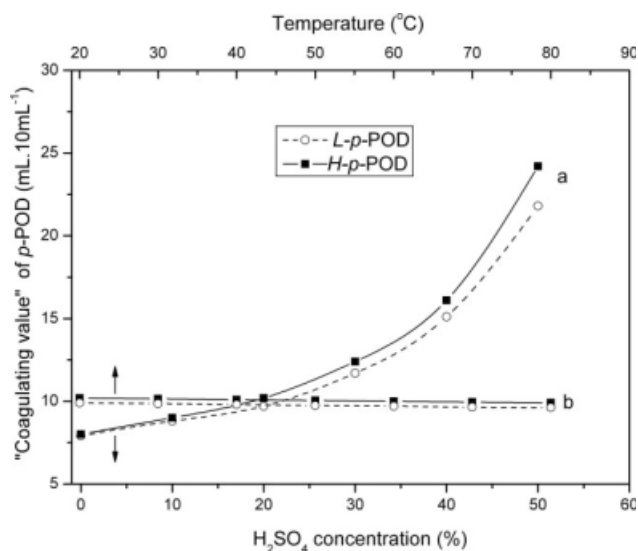


**Figure 1** The “coagulating value” of different H<sub>2</sub>SO<sub>4</sub> concentrations (a) and the same concentration (20%) at different temperatures (b) on different *p*-PODs.

which is 1.256 Km s<sup>-1</sup>, and *v*<sub>1</sub> is the velocities of the other samples measured.

Microscopic images were obtained by Scanning electron micrograph (SEM) of JSM-5900LV (JEOL) and high-definition microscope of Zeiss imager ZI and polarization microscope of 12Pol-S. To observe the skin-core structure conveniently, the fibers were colorized with disperse blue dye under 0.27 MPa

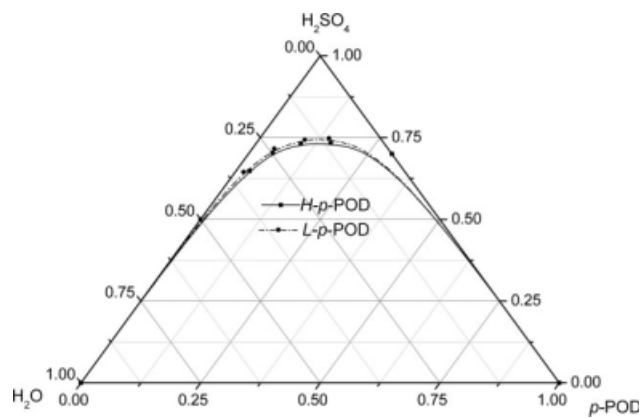


**Figure 2** Ternary phase diagrams of coagulation bath containing H<sub>2</sub>SO<sub>4</sub> and H<sub>2</sub>O with *p*-PODs at 50°C.

press at 130°C, and sliced for proportion analysis under the microscope.

The mechanical properties were characterized with single fiber electronic tensile strength tester. The fiber density was detected on MDMDY-350 density instrument (ZSMeidi instrument, China).

## RESULTS AND DISCUSSION

### Coagulability of sulfuric acids on different %CD *p*-PODs

The elemental analysis and intrinsic viscosity measurement results are listed in Table I. The elemental analysis indicates that the cyclization degree of the

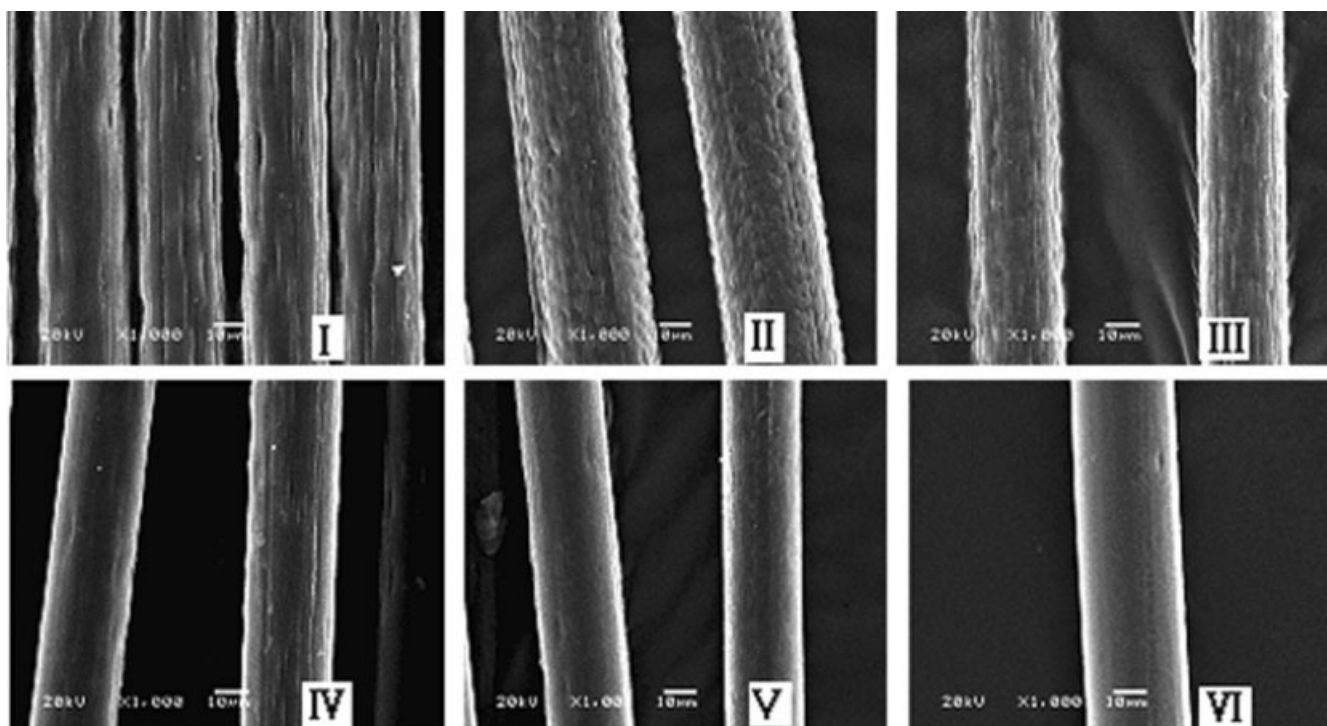


**Figure 3** The longitudinal SEM of *H-p*-POD as-spun fibers under different coagulating concentrations at 30°C (I, II, III, IV, V, VI stands for the fibers coagulated in 0, 10, 20, 30, 40, 50-wt% H<sub>2</sub>SO<sub>4</sub>, respectively).

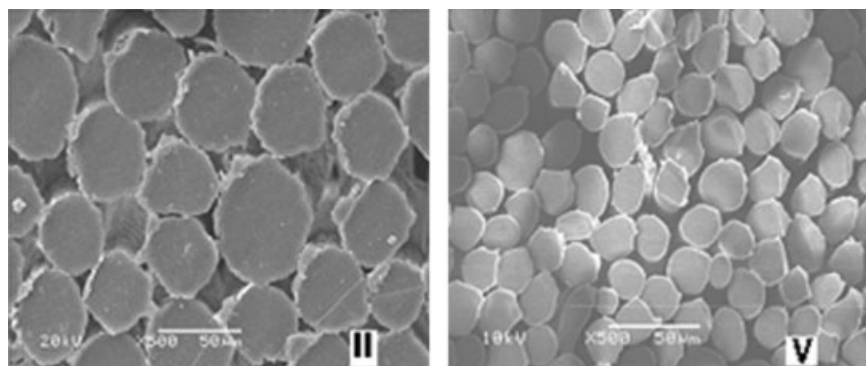


**Figure 4** The cross-section SEM of *H-p*-POD as-spun fibers under 10%(II) and 40%(V)  $\text{H}_2\text{SO}_4$  at  $30^\circ\text{C}$ .

*p*-PODs obtained via the novel one-step method is certainly enhanced, while the intrinsic viscosity does not decrease drastically.

The simplest and most representative parameter of the coagulability is the "coagulating value" which can be measured by the turbidity titration method.<sup>15</sup> So the coagulating values of the *p*-POD solutions at different sulfuric acid concentrations and bath temperatures were evaluated by that method. The values are shown in Figure 1(a,b). Figure 1(a) exhibits that the coagulating value of sulfuric acid on *L-p*-POD and *H-p*-POD increase with increasing  $\text{H}_2\text{SO}_4$  concentration from 0 to 50%. But the coagulating value of *H-p*-POD at the same acid concentration is slightly higher than that of *L-p*-POD, which indicates that *H-p*-POD is

more sensitive to sulfuric acid or difficult to coagulate at the same bath. This result is also verified by the ternary phase diagrams of the *p*-PODs (Fig. 2), in which the splitting phase area of *H-p*-POD is narrower than that of *L-p*-POD. With elevating temperature, the coagulating value slightly decreases [Fig. 1(b)], which indicates temperature has little effect on the coagulability of the *p*-POD solutions. A possible explanation is that the coagulation only depends on the thermodynamic phase behavior of the dilute polymer solution, but not on the dynamical double diffusion process of the real spinning solution.<sup>15</sup> The influences of  $\text{H}_2\text{SO}_4$  concentration and temperature on the fiber morphologic formation and mechanical properties will be discussed in another section of this article.

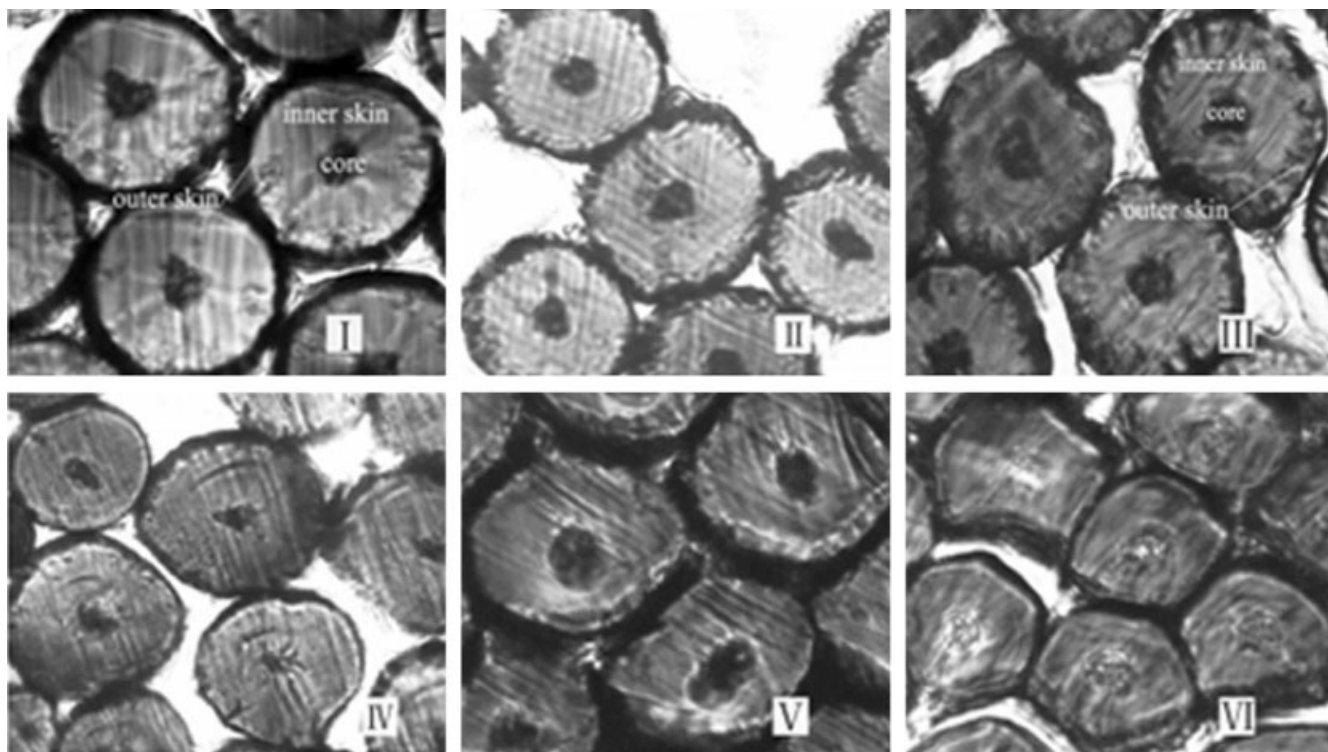


**Figure 5** The cross-section micrographs of *H-p*-POD as-spun fibers under different coagulating concentrations (I, II, III, IV, V, VI is the same as Figure 3 shows) at  $30^\circ\text{C}$ .

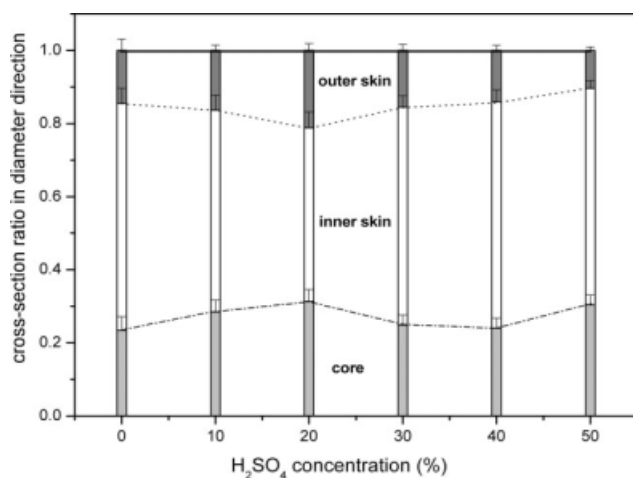


**Figure 6** The radial thickness variation of *H-p*-POD fibers coagulated by different H<sub>2</sub>SO<sub>4</sub> bath at 30°C.

**Morphological structure formation in different coagulating conditions**

The morphological structures of the *p*-POD as-spun fibers coagulated in different H<sub>2</sub>SO<sub>4</sub> baths were observed by SEM. Figures 3 and 4 are the longitudinal and cross-section SEM graphs of the *H-p*-POD as-spun fibers under different sulfuric acid concentrations from 0–50%. As shown in Figure 3, when the concentration of sulfuric acid increases from 0 to 20%, the surface feature of the as-spun fibers becomes smoother, the amplitude of the wrinkles or grooves on the fibers’ surface diminishes, and the intensity of the wrinkles becomes slight. However, effects of sulfuric acid concentrations on surface feature of the fibers gradually weakens when the sulfuric acid concentration increases from 30 to 50%. Figure 4 shows that the cross section of the as-spun fibers are dense and nearly round in shape when the coagulating bath is water, but becomes more irregular when H<sub>2</sub>SO<sub>4</sub> concentration is higher (up to 40%)

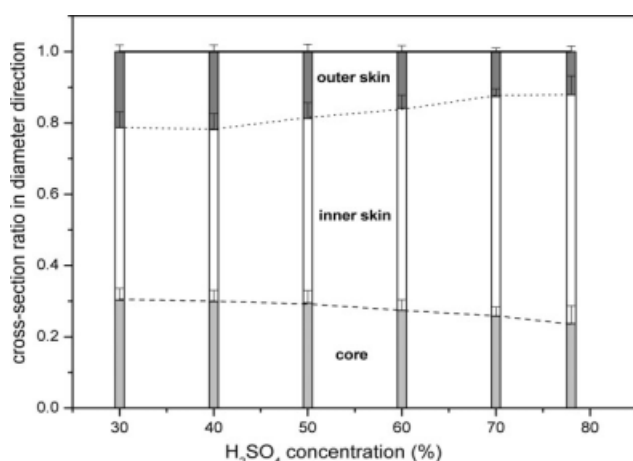


**Figure 7** The radial thickness variation of *H-p*-POD fibers coagulated by 20% H<sub>2</sub>SO<sub>4</sub> at different temperature.

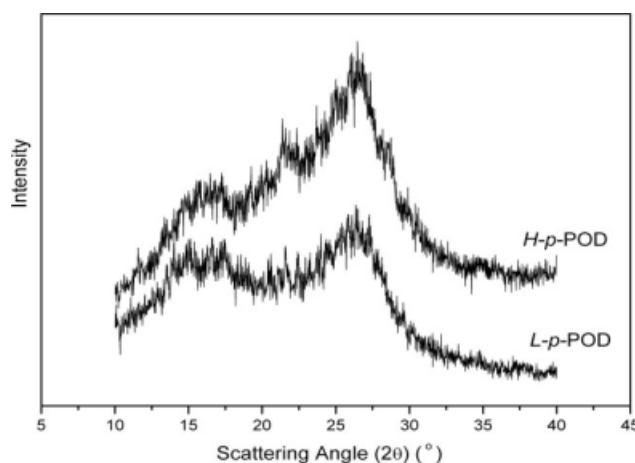


**Figure 8** X-ray diffraction patterns of *H-p*-POD powder coagulated in water.

because the weaker coagulability leads to softer skin which tends to be deformed.

Further observation of the as-spun fibers coagulated by different H<sub>2</sub>SO<sub>4</sub> baths was conducted with high-definition microscope after using a blue dye in the specified condition, and these images are shown in Figure 5. The images indicate the morphological architectures of all the as-spun fibers are of three-layer structure, which includes outer skin, inner skin, and the core. The images also illustrate that the shapes of cross section of the fibers are nearly circular when the H<sub>2</sub>SO<sub>4</sub> concentration is lower than 30%, but becomes more irregular with the increase of H<sub>2</sub>SO<sub>4</sub> concentration up to 40%. The results are similar to what is shown in Figure 4. The images in Figures 4 and 5 imply that the outer skin of the *H-p*-POD fiber turns from hard to soft as the H<sub>2</sub>SO<sub>4</sub> concentration increases. The radial thickness of each layer was calculated on the base of Figure 5, which is presented in Figure 6. The results demonstrate

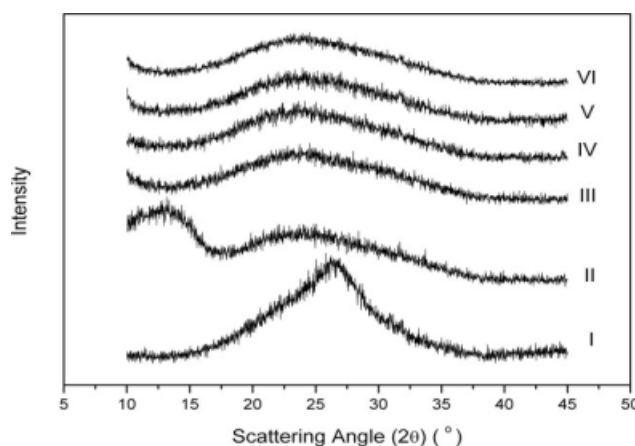


**Figure 9** X-ray diffraction patterns of *H-p*-POD as-spun fibers coagulated by different H<sub>2</sub>SO<sub>4</sub> bath at 30°C (I, II, III, IV, V, VI is the same as shown in Fig. 3).

**TABLE II**  
WAXD Structural Parameters for *p*-POD Powder and Fiber Coagulated in Water

Samples		$2\theta$ ( $^\circ$ )	$d$ (nm)	Height (cts)	Attribute of peaks
Powder coagulated in water	<i>H-p</i> -POD	22.22	0.400	23.4	Crystalline
		26.87	0.332	155.7	Crystalline
	<i>L-p</i> -POD	21.89	0.406	86.7	Crystalline
		26.61	0.335	259.6	Crystalline
Fiber coagulated in water	<i>H-p</i> -POD	22.41	0.397	204.8	Crystalline
		26.39	0.338	430.3	Amorphous

that the radial thickness of outer skin, inner skin, and the core varies with the change of  $\text{H}_2\text{SO}_4$  concentrations. For *H-p*-POD, the core size increases at first and then decreases when the  $\text{H}_2\text{SO}_4$  concentration increases from 0 to 40%, and the same trend has been observed for *L-p*-POD. The thickness variation of the outer skin for *H-p*-POD and *L-p*-POD with different  $\text{H}_2\text{SO}_4$  concentrations is also similar to that of the core. The morphology difference between the skin and the core of the fibers was further clarified by color difference of the cross section. The results indicate that the core is looser and easier to be colorized in darkness, and the inner skin which accounts for the most part of the cross section is denser and harder to be colorized, while the outer skin is the densest and hardest to be colorized.

The effect of coagulation temperature on the morphological structures of the *H-p*-POD fibers was also investigated by SEM and optical microscope (Fig. 7). With the bath temperature changing from 30 to 78°C, the surface of the fibers (coagulated in 20%  $\text{H}_2\text{SO}_4$ ) becomes smoother, and the cross section turns to be round and regular, and the section of the core and outer skin gets smaller. This is mainly due to the double-diffusion enhancement between the nonsolvent and solvent with increasing temperature, and the faster movement of water entering the fibers than that of sulfuric acid exiting from them.

#### Aggregation states of fibers coagulated in different baths

The effects of coagulation conditions on crystallinity of the *p*-POD powder and as-spun fibers were characterized by WAXD (Figures 8 and 9). The diffracto-

grams in Figure 8 indicate the formation of crystal structures, resulting from exothermic reaction and nonsolvent inducing crystallization when the hot *p*-POD solution (80–90°C) was poured into excess water at room temperature, and they also indicate that *H-p*-POD is prone to crystallization. The WAXD patterns in Figure 9 show the as-spun fibers change from crystalline to amorphous with increasing  $\text{H}_2\text{SO}_4$  concentration from 0 to 50%. To compare the crystal structure of the fibers with the powder coagulated in water, the data of two scattering peaks are listed in the Table II. The scattering angles ( $2\theta$ ) of the peaks position represent that the crystal structures induced by water are consistent with the results of Calandrelli.<sup>16</sup> The cross polarized light micrographs, which are shown in Figure 10, indicate birefringence patterns coming from both the orientation and crystal structures<sup>16</sup> of the as-spun fibers coagulated in water and 20%  $\text{H}_2\text{SO}_4$ , but the birefringence disappears for the as-spun fibers coagulated in 40%  $\text{H}_2\text{SO}_4$ . It is interesting that the whole cross section of the as-spun fibers coagulated in water shows the birefringence pattern and Maltese cross, suggesting the formation of spherulitic crystals both in the core and the skin. For the as-spun fibers coagulated in 20%  $\text{H}_2\text{SO}_4$ , only the outer skin layer displays the birefringence pattern. Nonbirefringence pattern is observed for the as-spun fibers coagulated in 40%  $\text{H}_2\text{SO}_4$ .

The X-ray diffraction graphs of the *H-p*-POD as-spun fibers coagulated in 20%  $\text{H}_2\text{SO}_4$  at different temperatures are shown in Figure 11. The patterns show that only broad amorphous halos appear for every sample, indicating that temperature has no obvious effect on coagulation of the *p*-PODs.

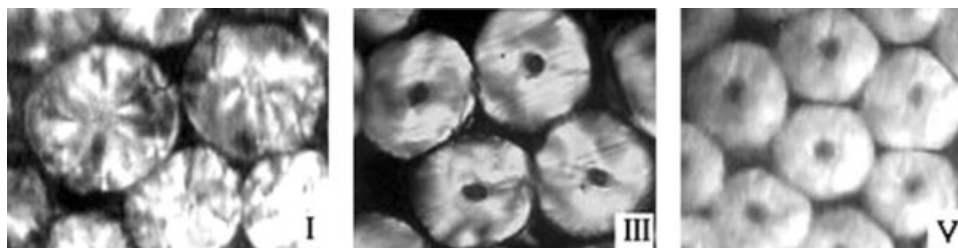


**Figure 10** The cross-section polar micrographs of *H-p*-POD as-spun fibers under different  $\text{H}_2\text{SO}_4$  concentrations at 30°C (I, III, V is the same as Figure 3 shows).

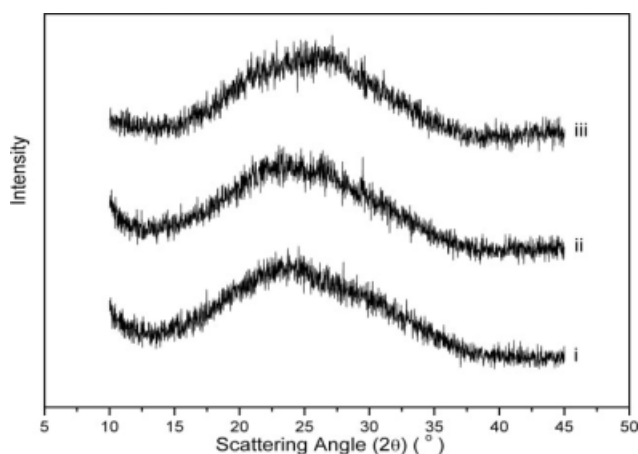


**Figure 11** X-ray diffraction patterns of *H-p*-POD as-spun fibers coagulated by 30°C (i), 50°C (ii), and 70°C (iii) 20% H<sub>2</sub>SO<sub>4</sub> bath.

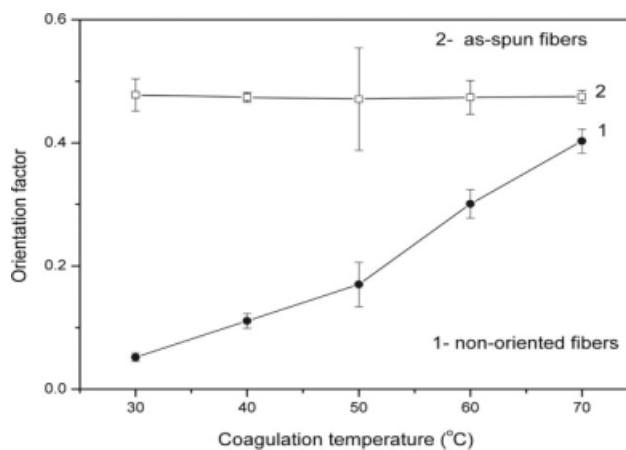


**Figure 13** Orientation factors of *H-p*-POD as-spun fibers coagulated in 20% H<sub>2</sub>SO<sub>4</sub> at different temperatures.

In the wet spinning process, the orientation of the *p*-POD molecular chain existed owing to the strong shearing stress and quick coagulation when the *p*-POD solution was extruded from the spinneret holes into the coagulation bath. It has been shown that ultrasonic wave propagation is sensitive to the morphology of the polymeric material and it increases markedly with the crystallinity according to the theory of two system,<sup>14,17,18</sup> whereas the X-ray pattern is not sensitive to the low crystalline polymers, and thus not proper to be characterized by minor orientation changes.<sup>17</sup> The ultrasonic velocities of the *p*-POD fibers were measured by the ultrasonic orientation measurement apparatus, and the orientation factors were calculated by eq. (2). Figure 12 demonstrates that the orientation factors of the as-spun fibers obtained in different H<sub>2</sub>SO<sub>4</sub> baths at 30°C decrease with increasing H<sub>2</sub>SO<sub>4</sub> concentration with the exception of the fibers obtained in 50% H<sub>2</sub>SO<sub>4</sub>. This is probably due to the unexpected stretching in

the spinning because of the soft and weak nature of the as-spun fibers. The dependence of the orientation factors of the nonoriented samples is much different from that of the as-spun fibers, for which the orientation factors go down at first and then go up with the increase of H<sub>2</sub>SO<sub>4</sub> concentration. However, it is clear that the orientation factors of the as-spun fibers are higher than that of the corresponding nonoriented samples. It is mainly due to more orientation of molecular chains under tension in coagulating bath. The higher orientation factors of the fibers coagulated in water and 10% H<sub>2</sub>SO<sub>4</sub> may be caused by quick coagulation and partial crystallinity. The changes of solid state structure of nonoriented samples from loose and irregular into compact and perfect structure lead to the increase of orientation factor, with H<sub>2</sub>SO<sub>4</sub> concentration increasing from 20 to 50%. The influences of temperature on the orientation factor of the as-spun fibers and nonoriented samples are shown in Figure 13, which demonstrates that temperature has little effect on the orientation

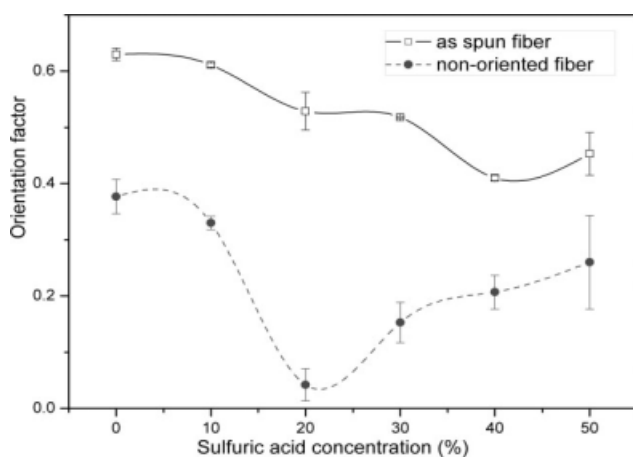


**Figure 12** Orientation factors of *H-p*-POD as-spun fibers coagulated in different H<sub>2</sub>SO<sub>4</sub> baths at 30°C.

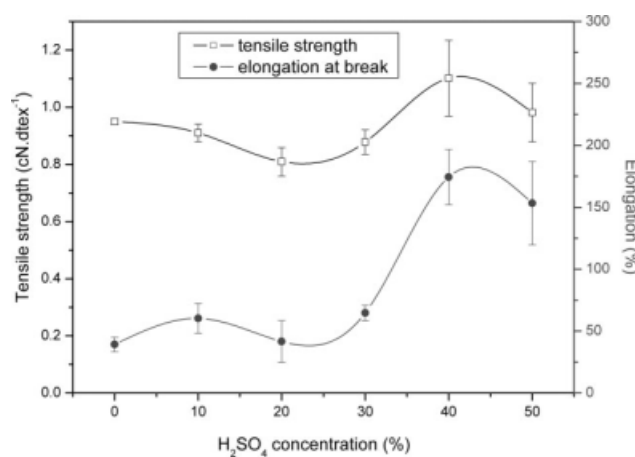


**Figure 14** Tensile properties of *H-p*-POD as-spun fibers coagulated in different H<sub>2</sub>SO<sub>4</sub> baths at 30°C.

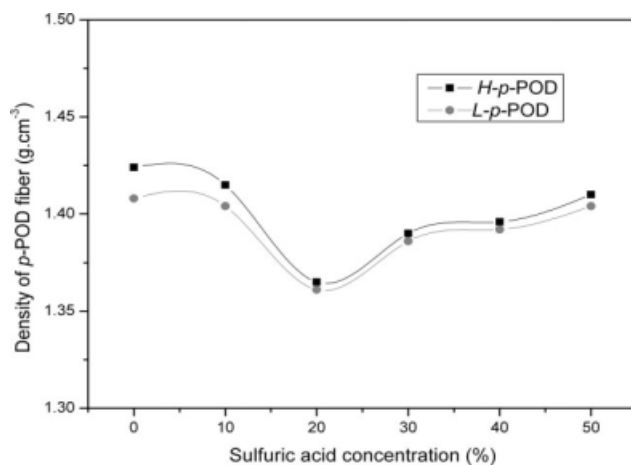


**Figure 15** Variation of the density of as-spun fibers coagulated in different  $\text{H}_2\text{SO}_4$  baths at  $30^\circ\text{C}$ .

factor of the as-spun fibers, but great influence on the nonoriented samples in the course of the enhancing of coagulability.

#### Mechanical properties and post processabilities of as-spun fibers

The change of tensile properties with sulfuric acid concentration reflects the coagulability and solid structure of fibers. The effect of sulfuric acid concentration on the tensile properties of the as-spun fibers is presented in Figure 14. The tensile strength of the *H-p*-POD fibers drops down at first, then increases, and drops again with increase in sulfuric acid concentration from 0 to 50%. The *L-p*-POD fibers also follow a similar trend. The lowest tensile strength and elongation at break appear in 20%  $\text{H}_2\text{SO}_4$  because of the poor solid structure. When the concentration of  $\text{H}_2\text{SO}_4$  is up to 30%, the abrupt drop of coagulability leads to the formation of the perfect morphology, which is in accordance with the analytical results of

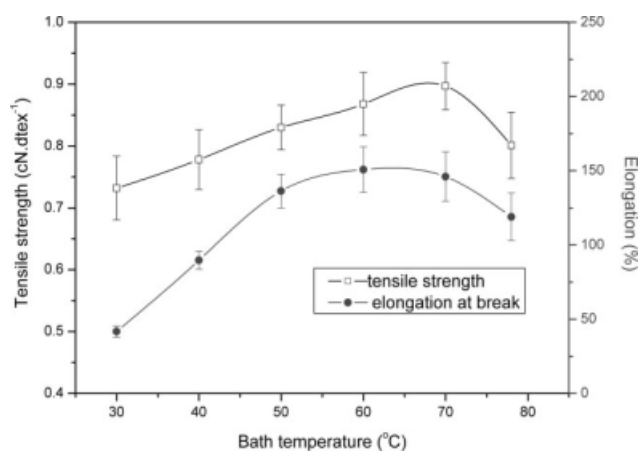


**Figure 16** Tensile properties of *H-p*-POD as-spun fibers coagulated in 20%  $\text{H}_2\text{SO}_4$  at different temperatures.

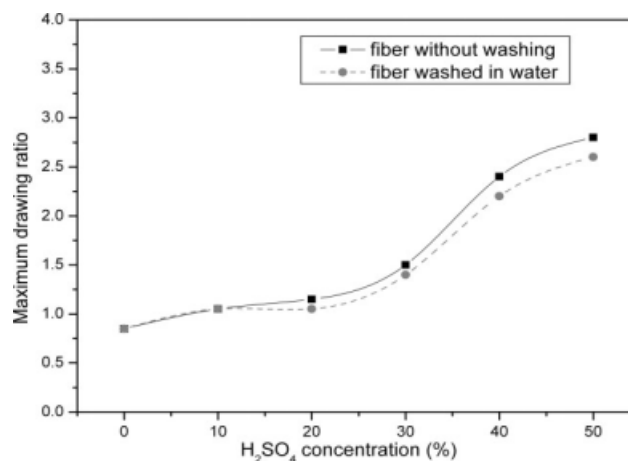


**Figure 17** Maximum drawing ratios of *H-p*-POD as-spun fiber coagulated in different  $\text{H}_2\text{SO}_4$  baths at  $30^\circ\text{C}$ .

orientation and crystallinity. This conclusion is further verified by the density measurement as shown in Figure 15.

The influences of the temperature on the tensile properties of the *p*-POD fibers are presented in Figure 16. It shows that the coagulation temperature does not affect the tensile strength, but affects the elongation. The elongation at break increases with increasing temperature except for the point near the spinning solution temperature (about  $80^\circ\text{C}$ ).

It is well known that the mechanical properties and morphological structure influence the post-processabilities of the as-spun fibers and the end properties of the final products. The maximum drawing ratios of the as-spun fibers before and after washing are compared in Figures 17 and 18. The results of the stretching experiment indicate that the maximum drawing ratios of the unwashed fibers are higher than the washed ones. In combination with the results of Figures 15 and 16, it is concluded that the post-stretching process for the fibers prepared in

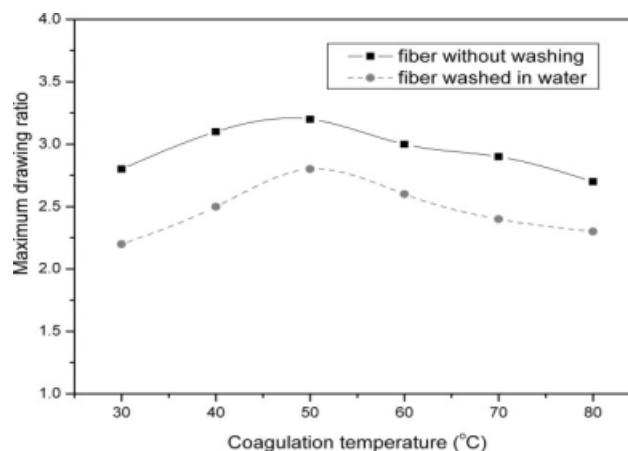


**Figure 18** Maximum drawing ratios of *H-p*-POD as-spun fiber coagulated in 45%  $\text{H}_2\text{SO}_4$  at different temperatures.



the optimal coagulation process (coagulated in 45% H<sub>2</sub>SO<sub>4</sub> at around 50°C) would be carried out under acid conditions at a specified temperature.

Besides the optimal temperature and concentration, adequate coagulating time is also necessary for obtaining good mechanical properties of the fibers. The further study on the double diffusion process of the as-spun fibers coagulated in 45% H<sub>2</sub>SO<sub>4</sub> at 50°C shows that the equilibrium of the diffusion balance of the nonsolvent (water) and solvent (H<sub>2</sub>SO<sub>4</sub>) can be reached at about 10 s (as seen in Fig. 19), suggesting that the coagulating time should be more than 10 s.

The tensile properties of the *L-p*-POD and *H-p*-POD fibers after being stretched and heat treatment are listed in Table III. The data illustrates that the *L-p*-POD fibers have higher tensile strength, lower initial modulus, and density, because their flexible chains can be easily oriented but difficult to crystallize. It also exhibits higher elongation at break and higher moisture retention than that of the *H-p*-POD fibers. It should be noted that the *p*-POD fibers are not suitable for heat-stretching and can only be heat-treated under tension because of its high glass transition temperature ( $T_g$ ).

## CONCLUSIONS

Poly(*p*-phenylene-1,3,4-oxadiazoles) solutions prepared by one-step polycondensation were extruded into different sulfuric acid coagulation baths to form the as-spun fibers. The structure and mechanical properties of the *p*-POD fibers are largely affected by their cyclization degrees and the coagulation conditions. As the coagulation composition and temperature vary, the morphologies and the mechanical properties of the as-spun fibers change greatly. Generally, three conclusions can be drawn from the discussions above. Firstly, the *p*-POD as-spun fibers

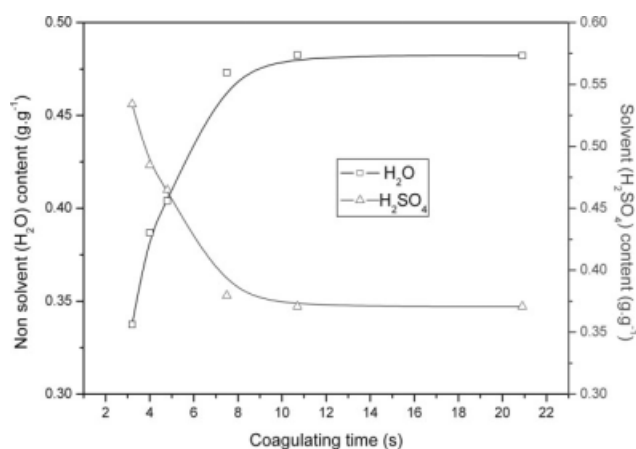


**Figure 19** Variation of solvent and nonsolvent content of as-spun fibers coagulated in 45% H<sub>2</sub>SO<sub>4</sub> bath at 50°C with coagulating time.

**TABLE III**  
Properties of *p*-POD Fibers Spun in 45% H<sub>2</sub>SO<sub>4</sub> Bath at 50°C

	<i>L-p</i> -POD fiber	<i>H-p</i> -POD fiber
[ $\eta$ ] (dL g <sup>-1</sup> )	1.89	1.69
Cyclization degree (%)	59.7	76.5
Maximum stretch ratio	4.2	3.5
Orientation factor	0.81	0.88
Linear density (dtex)	2.3	2.6
Tenacity (cN dtex <sup>-1</sup> )	3.5	3.2
Elongation at break (%)	30.5	22.4
Initial modulus (cN dtex <sup>-1</sup> )	87.5	110.4
Density (g cm <sup>-3</sup> )	1.42	1.43
Moisture regain (in 70% RH at 22°C) (%)	8.7	5.5
Maximum heat stretch ratio at 300–450°C	≤1.1	≤1.05

have three-layer skin-core structure. The surface feature, cross section shape, and the radial thickness are significantly affected by bath conditions. Secondly, with variation of the bath conditions, the crystallinity, and the orientation of the fibers also change apparently. Nonsolvents can induce crystallization of *p*-PODs, and higher solvent content and suitable temperature of the bath can lead to denser and more regular structure. Finally, appropriate coagulation condition is in favor of higher compaction, and eventually the improvement of the fiber's mechanical properties.

## References

- Schulz, B.; Bruma, M.; Brehmer, L. *Adv Mater* 1997, 9, 601.
- Klyueva, V. V.; Tsarev, I. V.; Pushkina, A. A.; Degtyareva, L. S.; et al. U.S.S.R. Pat. SU 1,346,199 (1981).
- Lozinskaya, E. I.; Shaplov, A. S.; Kotseruba, M. V.; Komarova, L. I.; et al. *J Polym Sci Part A: Polym Chem* 2006, 44, 380.
- Schulz, B.; Eibnitz, E. L. *Acta Polym* 1992, 43, 343.
- Frazer, A. H.; Wallenberger, F. T.; et al. *J Polym Sci Part A: Polym Chem* 1964, 2, 1137.
- Iwakura, Y.; Uno, K.; Hara, S. *J Polym Sci Part A: Polym Chem* 1965, 3, 45.
- Ueda, M.; Sugita, H. *J Polym Sci Part A: Polym Chem* 1988, 26, 159.
- Milkova, L. P.; Romanov, V. V.; Poshalkin, N. S.; Krucinin, N. P.; et al. *Volokna* 1986, 3, 32.
- Imai, Y. *J Appl Polym Sci* 1970, 14, 225.
- Varma, S. K.; Geetha, C. K.; Khandedwal, B. L.; et al. *J Appl Polym Sci* 1981, 26, 571.
- Jones, R. S.; Soehngen, J. W. *J Appl Polym Sci* 1980, 25, 315.
- Hofmann, D.; Leibnitz, E.; Schmolke, R.; Schulz, B. *Die Angew Makromol Chem* 1993, 204, 111.
- Zhang, Z. X.; Li, W. T.; Ye, G. D.; Xu, J. J. *Plast Rubber Compos* 2007, 36, 343.
- Moseley, W. W., Jr. *J Appl Polym Sci* 1960, 3, 266.
- Ziabicki, A. *Fundamentals of Fiber Formation*; Wiley: London, 1976.
- Calandrelli, L.; Immirzi, B.; Malinconico, M.; Martuscelli, E.; et al. *Makromol Chem* 1990, 191, 2537.
- Samules, R. J. *Structure Polymer Properties—The Identification, Interpretation and Application of Crystalline Polymer Structure*; Wiley: London, 1974.
- Tanaka, A.; Nitta, K. H. *Polym Eng Sci* 1991, 31, 571.